Assimilation of Satellite Albedo to Improve Simulations of Glacier Hydrology

André Bertoncini[1] and John Pomeroy[1]

[1]University of Saskatchewan

March 24, 2024

Abstract

Wildfires and heatwaves have recently affected the hydrological system in unprecedented ways due to climate change. In cold regions, these extremes cause rapid reductions in snow and ice albedo due to soot deposition and unseasonal melt. Snow and ice albedo dynamics control net shortwave radiation and the available energy for melt and runoff generation. Many albedo algorithms in hydrological models cannot accurately simulate albedo dynamics because they were developed or parameterised based on historical observations. Remotely sensed albedo data assimilation (DA) can potentially improve model performance by updating modelled albedo with observations. This study seeks to diagnose the effects of remotely sensed snow and ice albedo DA on the prediction of streamflow from glacierized basins during wildfires and heatwaves. Sentinel-2 20-m albedo estimates were assimilated into a glacio-hydrological model created using the Cold Regions Hydrological Modelling Platform (CRHM) in two Canadian Rockies glacierized basins, Athabasca Glacier Research Basin (AGRB) and Peyto Glacier Research Basin (PGRB). The study was conducted in 2018 (wildfires), 2019 (soot/algae), 2020 (normal), and 2021 (heatwaves). DA was employed to assimilate albedo into CRHM to simulate streamflow and was compared to a control run (CTRL) using off-the-shelf albedo parameters. Albedo DA benefited streamflow predictions during wildfires for both basins, with a KGE coefficient improvement of 0.18 and 0.20 in AGRB and PGRB, respectively. Four-year DA streamflow predictions were superior to CTRL in PGRB, but DA was slightly better in AGRB. DA was not beneficial to streamflow predictions during heatwaves. These results show that albedo DA can reveal otherwise unknown albedo and snowpack dynamics occurring in remote glacier accumulation zones that are not well simulated by model predictions alone. These findings corroborate the power of observational tools to incorporate near real-time information into hydrological models to better inform water managers of the streamflow response to wildfires and heatwaves.

Assimilation of Satellite Albedo to Improve Simulations of Glacier Hydrology

André Bertoncini[a] and John W. Pomeroy[a]

[a]*Centre for Hydrology, University of Saskatchewan, Canmore, Alberta, Canada*

Corresponding author : André Bertoncini, andre.bertoncini@usask.ca

Co-author e-mail : John W. Pomeroy, john.pomeroy@usask.ca

Data Availability Statement

MODIS, Sentinel-2, and ERA5-Land data can all be found in the GEE platform. Forcing and evaluation data, as well as the Python codes for computing the remotely sensed albedos and R codes to perform the EnKF DA can be found at:*https://github.com/andrebertoncini/albedo_data_assimilation*.

Funding Statement

This work was supported by the Canada Research Chairs programme, the Natural Sciences and Engineering Research Council of Canada (NSERC), Alberta Innovates, and the Canada First Research Excellence Fund's

(CFREF) Global Water Futures programme.

Conflict of Interest Disclosure

We have no conflict of interest to disclose.

Abstract

Wildfires and heatwaves have recently affected the hydrological system in unprecedented ways due to climate change. In cold regions, these extremes cause rapid reductions in snow and ice albedo due to soot deposition and unseasonal melt. Snow and ice albedo dynamics control net shortwave radiation and the available energy for melt and runoff generation. Many albedo algorithms in hydrological models cannot accurately simulate albedo dynamics because they were developed or parameterised based on historical observations. Remotely sensed albedo data assimilation (DA) can potentially improve model performance by updating modelled albedo with observations. This study seeks to diagnose the effects of remotely sensed snow and ice albedo DA on the prediction of streamflow from glacierized basins during wildfires and heatwaves. Sentinel-2 20-m albedo estimates were assimilated into a glacio-hydrological model created using the Cold Regions Hydrological Modelling Platform (CRHM) in two Canadian Rockies glacierized basins, Athabasca Glacier Research Basin (AGRB) and Peyto Glacier Research Basin (PGRB). The study was conducted in 2018 (wildfires), 2019 (soot/algae), 2020 (normal), and 2021 (heatwaves). DA was employed to assimilate albedo into CRHM to simulate streamflow and was compared to a control run (CTRL) using off-the-shelf albedo parameters. Albedo DA benefited streamflow predictions during wildfires for both basins, with a KGE coefficient improvement of 0.18 and 0.20 in AGRB and PGRB, respectively. Four-year DA streamflow predictions were superior to CTRL in PGRB, but DA was slightly better in AGRB. DA was not beneficial to streamflow predictions during heatwaves. These results show that albedo DA can reveal otherwise unknown albedo and snowpack dynamics occurring in remote glacier accumulation zones that are not well simulated by model predictions alone. These findings corroborate the power of observational tools to incorporate near real-time information into hydrological models to better inform water managers of the streamflow response to wildfires and heatwaves.

Keywords: Albedo, Data Assimilation, Wildfires, Heatwaves, Cold Regions Hydrological Model (CRHM), Streamflow Prediction, Glacier Hydrology, Sentinel-2.

1. Introduction

In an era of global environmental change, hydrological models need to account for processes resulting from unprecedented combinations of forcing meteorology, state variables, and parameters. Although the hydrological community has made advances in creating physically based process hydrology models, many process representations are based on historical behaviour. Recent wildfires and heatwaves worldwide, especially in Canada (Baars *et al.* , 2019; Parisien *et al.* , 2023), challenge the calculation of net shortwave radiation using snow and ice albedo algorithms based on historical representations. Snow and ice surfaces can be darkened by wildfire soot deposition. Likewise, snow surfaces can be darkened by accelerated snowmelt caused by rapid above-average temperature changes from heatwaves. These two conditions strongly impact melt energy for the seasonal snowpack, perennial snowfields and mountain glaciers, resulting in faster melt than might be estimated without consideration of rapid surface darkening.

Shortwave (SW) radiation input into glacierized basins is often the most important source of available energy for melt and runoff generation. Albedo, therefore, controls the amount of SW radiation entering snow and ice surfaces and the availability of melt energy. The mechanism controlling snow and ice albedo decrease due to wildfire soot deposition is straightforward. It depends on the amount of soot deposited over a surface and whether or not that soot would be washout by melt or be further developed by algae growth (Aubry-Wake *et al.* , 2022a; Bertoncini *et al.* , 2022; Esser et al., accepted manuscript). Heatwaves, in contrast, have a more intricate effect on snow and ice albedo. Rapid above-temperature changes can cause accelerated snowmelt (Koboltschnig *et al.* , 2009; Box *et al.* , 2022) and consequently earlier exposure of firn and ice; however, these same high temperatures will most likely not further decrease the albedo of firn and ice in nature. It is unknown whether or not current hydrological model albedo algorithms are able to account for such different interplay of environmental conditions in a nonstationary changing climate, given they were developed and parameterised based on historical observations. Up-to-date albedo observations are, therefore, necessary to update hydrological model albedo algorithms. The availability of near real-time, high-resolution satellite data with shorter revisit times combined with the advancement of albedo retrieval algorithms has provided superior quality albedo data for effective assimilation into hydrological models.

Glacio-hydrological models are a set of numerical representations of hydrological processes that together culminate in the ability to predict surface water and energy budget terms, the states of soil moisture, groundwater storage, snowpacks, and glacier mass balance and fluxes of evaporation, sublimation, and streamflow. These models are forced with meteorological variables and parameterized with environmental information, and they can be used to simulate hydrologically-relevant variables such as snow water equivalent (SWE) (Wrzesien *et al.* , 2017; Marsh *et al.* , 2020) to unobserved locations or to diagnose previous flood (Hamlet and Lettenmaier, 2007; Pomeroy *et al.* , 2016) and drought (Fang and Pomeroy, 2007; Mishra and Singh, 2011) events. Numerical weather precipitation models can force hydrological models for short-term flood forecasting to prepare riverine communities for flooding (Alfieri *et al.* , 2013; Thieken *et al.* , 2023). Finally, climate projections coupled with hydrological models can guide governments and environmental planners regarding a region's future state of water resources (Milly *et al.* , 2002; Blöschl *et al.* , 2019). All these applications make hydrological modelling a crucial tool to learn from the past and prepare for short- and long-term changes in the hydrological cycle to avoid the large cost of floods and droughts. The global costs of floods and drought-related (plus heatwaves and wildfires) extreme events attributed to climate change amounts to US$ 127 billion per year between 2000 and 2019 (Newman and Noy, 2023).

There are three main types of hydrological models depending on the manner in which how hydrological processes are represented. These range from empirical, semi-empirical, to physically based hydrological models (Beven, 2012). Ideally models should represent hydrological processes as physically-based as possible (Paniconi and Putti, 2015); however, often inefficiencies in model physical processes development are masked by heavy calibration (Menard *et al.* , 2021). The physically based effort is a pledge to make hydrological models more robust to unprecedented environmental conditions (Kreibich *et al.* , 2022). Models that heavily rely on empiricism to represent hydrological processes are more likely to be deemed unsuccessful under conditions that have not been observed in the past. For instance, the uncertainty in end-of-century mean flows can be over 40% due to the choice of hydrological models of various degrees of physical process representation (Krysanova *et al.* , 2017). Moreover, these unprecedented environmental conditions will likely be more common under climate change-induced modifications in the overall hydrological system (Blöschl *et al.* , 2019; Queen *et al.* , 2021). Therefore, it is crucial that process representation in hydrological models be as physically based as possible for riverine communities to be prepared for upcoming extreme hydrological events. However, developing robust physical process representation is time-consuming. In the meantime, other techniques should be explored to account for inherent process representation inefficiencies that are still represented semi-empirically in physically based models (Beven, 2012).

One way to correct for the lack of physical representation in hydrological modelling is through DA. In simple terms, DA tries to create an optimal estimate ($\hat{x}$) of a true real-world state (x) by combining a modelled state (m) and a corresponding observation (o). The optimal state $\hat{x}$ is a weighted sum of$m$ and o. The weights are defined by the uncertainty in m and$o$, favouring the less uncertain estimate of $\hat{x}$. The observation uncertainty, or measurement error, is usually defined a priori based on the literature or ground-truthing. On the other hand, the modelling error can be determined using many available techniques, which are usually based on some sort of Monte Carlo simulations that can capture the spread in multiple model trajectories (Reichle, 2008). The most commonly used technique in hydrology and snow modelling is the Ensemble Kalman Filter (EnKF) (Andreadis and Lettenmaier, 2006; Clark*et al.* , 2006, 2008; Slater and Clark, 2006; Huang *et al.* , 2017; Lv and Pomeroy, 2020), which is a less computationally expensive version of the previously developed Extended Kalman Filter (EKF) (Reichle *et al.* , 2002). The EnKF method calculates the modelling error based on an ensemble of simulated model states forced by perturbed variables. The simulations are carried out until the most recent available observation. Then, the Kalman gain is calculated, allowing the optimal state estimate to be calculated and replaced in the model for future simulations (Evensen, 1994). The EnKF is advantageous against other smoothing DA techniques because it can be implemented in a forecasting mode by calculating modelling error using only one available observation (Reichle, 2008). This EnKF characteristic is suitable for improving streamflow forecasting systems (Huang *et al.* , 2017). Among many snow and hydrology variables, remotely sensed albedo DA has been utilized in large-scale land surface models (LSMs) to estimate SWE (Dumont *et al.* , 2012; Malik *et al.* , 2012; Wang *et al.* , 2015), but not yet in a full hydrological model capable of predicting streamflow.

Some hydrological models, especially those dedicated to the simulation of snow and ice processes important to cold regions, have a dynamic albedo simulation algorithm. Accurate simulation of albedo is critical to define the net shortwave radiation of snowpacks and glaciers, as shortwave radiation is the primary source of available energy for melt. Albedo algorithms intend to simulate temporal changes in surface albedo within a spatial modelling unit arising from soil moisture variations, vegetation phenology, addition of fresh snow cover, snow depletion, and firn and glacier ice exposure. In the case of partially or completely covered snowpacks, the albedo varies due to solar angle diurnal and seasonal variations, snow grain size (Marks and Dozier, 1992), the amount of snow-free surfaces (Pomeroy *et al.* , 1998), and the amount of light-absorbing particles (LAPs) in snow (Warren and Wiscombe, 1980). Empirical snow albedo estimation algorithms have been developed and applied satisfactorily in the past (Gray and Landine, 1987; Verseghy, 2012); however, the conditions to which they were developed have changed drastically with climate change. In the case of bare ground and short vegetation, these algorithms usually apply a constant known albedo for fresh snow and a decay function until it reaches a depth in which the snow-free albedo starts to contribute, and ultimately, a constant snow-free albedo is used. The albedo is reset when fresh snow accumulates on the ground, and the decay function starts again. Physically based radiative transfer algorithms have been developed to simulate snow and ice albedo (Wiscombe and Warren, 1980; Gardner and Sharp, 2010). Some of these physically based algorithms can also account for the introduction of LAPs into the snowpack (Zhang *et al.* , 2017; McKenzie Skiles *et al.* , 2018). Although these physically based algorithms should be more robust in their ability to estimate albedo in a changing climate with more wildfires and heatwaves, they are usually complex and, therefore, rarely implemented in hydrological models (Pietroniro *et al.* , 2007; Bergström and Lindström, 2015; Hamman *et al.* , 2018; Pomeroy *et al.* , 2022), especially algorithms capable of accounting for LAPs deposition. Studies usually determine the LAPs radiate forcing and its respective melt, but are unable to directly couple them into a hydrological model (Flanner*et al.* , 2007; Zhang *et al.* , 2017; McKenzie Skiles *et al.* , 2018; Magalhães *et al.* , 2019), unless the model is directly forced by albedo observations (Aubry-Wake *et al.* , 2022a).

Albedo can also be estimated using remotely sensed imagery. Spectral albedo can be simply calculated by dividing the reflected spectral radiance by the incoming solar radiation at the surface for a given region of the solar electromagnetic spectrum. Besides hyperspectral sensors, most remote sensing systems only have a few narrow spectral bands, and a conversion to the full broadband solar spectrum is necessary to calculate albedo. This conversion is usually done using narrow-to-broadband equations developed for the most common sensors using field spectroscopy libraries or radiative transfer simulations (Liang, 2000; Greuell *et al.* , 2002; Li *et al.* , 2018). In addition, because most high-resolution multi-spectral remote sensing systems operate at nadir viewing angles, they cannot observe albedo variations due to different sensor-solar geometries. One way to overcome that is to use coarse resolution systems with off-nadir capabilities, such as the Visible Infrared Imaging Radiometer Suite (VIIRS) or the Moderate Resolution Imaging Spectroradiometer (MODIS), to calculate a Bidirectional Reflectance Distribution Function (BRDF) (Roujean *et al.* , 1992; Wanner *et al.* , 1995; Li *et al.* , 2001). This BRDF information can be downscaled to Landsat-era (30-m) and Sentinel-2 (20-m) resolutions in soil and vegetation surfaces (Shuai *et al.* , 2011). These methodologies have been successfully applied for soil and vegetation surfaces, but they were suboptimal on snow and ice surfaces due to sensor saturation prior to the launch of Landsat-8. With the advancement in sensor radiometric technology onboard Landsat-8 and Sentinel-2 platforms, surface reflectance can be estimated over snow and ice at high-resolution and, in conjunction with BRDFs, calculate albedo over snow and ice (Wang *et al.* , 2016; Li *et al.* , 2018; Bertoncini *et al.* , 2022). The high revisit time of Sentinel-2 platforms has allowed such technologies to capture rapid snow and ice albedo changes caused by wildfire soot deposition and its associated SW radiative forcing (Bertoncini *et al.* , 2022).

The degree to which streamflow predictions during melt of snow and ice can be improved by high-resolution remotely sensed albedo DA into hydrological models has not been assessed yet. Given the importance of simulating accurate current and future streamflows and the increasing trends of unprecedented wildfire and heatwaves (Jolly *et al.* , 2015; Kirchmeier-Young *et al.* , 2019; Al-Yaari *et al.* , 2023; Parisien *et al.* , 2023), accounting for these unrepresented processes in glacio-hydrological models can be crucial. Because current hydrological model's albedo algorithms are not able to account for rapid and unseasonal snow and ice albedo changes (Pietroniro *et al.* , 2007; Bergström and Lindström, 2015; Hamman *et al.* , 2018; Pomeroy*et al.* , 2022; Wheater *et al.* , 2022), albedo DA provides a path forward in improving this process's representation. Modular physically based models such as CRHM (Pomeroy *et al.* , 2022) provide a suitable platform to test albedo DA in cold regions. Although coarse-resolution remotely sensed snow and ice albedo DA into LSMs has been performed to estimate SWE in the past (Dumont *et al.* , 2012; Malik *et al.* , 2012; Wang *et al.* , 2015), not until recently that high-resolution remotely sensed snow and ice albedo estimates became reliable and frequent enough (Li *et al.* , 2018; Bertoncini*et al.* , 2022) to have an impact on hydrological model streamflow predictions. Therefore, no studies have assessed the impact of remotely sensed high-resolution albedo DA into a cold regions hydrological model on streamflow predictions during extreme wildfire and heatwave conditions, especially in glacierized mountain headwater basins.

The purpose of this chapter is to diagnose the effects of remotely sensed high-resolution snow and ice albedo data assimilation on the prediction of streamflow of high mountain glacierized basins during wildfires and heatwaves. The specific objectives are (i) to develop and evaluate a cloud-computing remotely sensed snow and ice albedo retrieval framework, (ii) to develop a framework for remotely sensed albedo DA into a physically-based cold regions hydrological model, and (iii) to assess the impact of albedo DA on streamflow prediction of glacierized basins during wildfire and heatwave conditions. The albedo DA framework was developed and tested in the Athabasca Glacier and Peyto Glacier research basins in the Canadian Rockies during contrasting environmental conditions that included wildfires and heatwaves between the 2018 and 2021 water years (WYs). The framework was developed based on 20-m Sentinel-2 imagery albedo estimates that were assimilated into CRHM to assess the impact of wildfires and heatwaves on streamflow predictions.

2. Material and Methods

2.1. Study Area

Two glacierized basins in the Canadian Rockies, Alberta, were used as study areas for this research: Athabasca Glacier and Peyto Glacier research basins (Figure 1). AGRB is in Jasper National Park and is part of the Global Water Futures Observatory (GWFO) and operated by the Centre for Hydrology, University of Saskatchewan. AGBR is a glacier outlet of the Columbia Icefield, the largest icefield in the Canadian Rockies and a triple continental drainage divide between the Mackenzie, Nelson, and Columbia river basins which flow into the Arctic, Atlantic, and Pacific oceans, respectively. AGBR has an area of 29.3 km^2 and sits between 1926 and 3459 m of elevation (as of 2011), with 58% of its area covered by glacier ice (as of 2016) (Pradhananga and Pomeroy, 2022). AGBR is equipped with two automatic weather stations (AWS), Athabasca Ice and Athabasca Moraine, and one streamflow gauge. PGRB drains into the Nelson river basin. PGRB has an area of 22.4 km^2 and sits between 1907 and 3152 m (as of 2014), with 44% of its area covered by glacier ice (as of 2016) (Pradhananga and Pomeroy, 2022). PGRB has one AWS (Peyto Main) and a streamflow gauge and has been the subject of intense scientific studies since the 1960s. For more information about these research basins and their instruments the readers are referred to Pradhananga *et al.*(2021) and Pradhananga and Pomeroy (2022).

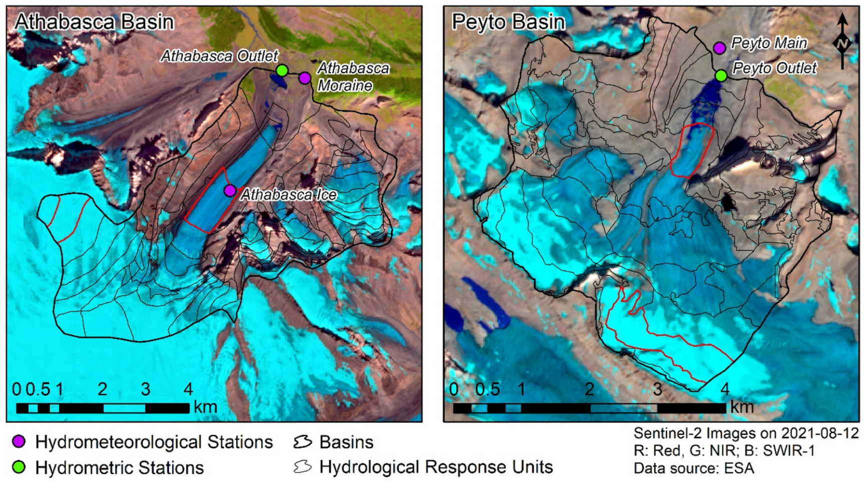

Figure 1: Athabasca Glacier Research Basin (AGRB, left) and Peyto Glacier Research Basin (PGRB, right) study areas in the Canadian Rockies, Alberta. Glacier ice and snow Hydrological Response Units (HRUs) used as examples for result discussions are highlighted in red.

2.2. Study Period and Environmental Conditions

The study was conducted between July 2017 and September 2021, and streamflow evaluation was performed for the four complete WYs inside this period (2018, 2019, 2020, and 2021). The 2018 year was the worst interior British Columbia wildfire season to date (Parisien *et al.* , 2023) – as these fires were generally upwind of the study basins they impacted the sites with smoke and soot deposition (Aubrey-Wake*et al.* , 2022). The 2019 year did not have any major wildfires; however, field inspections revealed that albedo remained low in the Athabasca Glacier from soot and algae growth feeding off soot deposited in 2017 and 2018 (Aubry-Wake *et al.* , 2022a; Bertoncini *et al.* , 2022; Esser *et al.* , accepted manuscript). The 2020 year had no major wildfires and can be considered a control year with greatly reduced soot and algae. The 2021 year was characterized by intense heat and an unprecedented heat dome that dominated the region for many days in late June and early July (Lin *et al.* , 2022). Although there was also a considerable Western Canada wildfire season in 2021, only light smoke was observed in the study basins; therefore, this year was not considered a high-activity wildfire season. The 2017 year was also a high-activity wildfire season. However, DA evaluation was not performed in that year because Sentinel-2B satellite images were only available from July 2017 onwards and thus not spanning the whole glacier ablation period. The Sentinel-2B satellite launch conferred high revisit rates every 2 to 5 days in the region.

2.3. Cloud-computing Remotely Sensed Albedo Framework Implementation

High-resolution remotely sensed albedo was estimated using a framework developed by Shuai *et al.* (2011) for Landsat images, updated by Li *et al.* (2018) for Sentinel-2 images, and applied by Bertoncini*et al.* (2022) in the Columbia Icefield to assess the impacts of wildfires on albedo and net SW radiation. To extend the application for use in hydrological models, Bertoncini *et al.* (2022)'s framework was implemented in the Google Earth Engine (GEE) cloud-computing platform. The algorithm was slightly modified to run in GEE. The main differences from Bertoncini *et al.* (2022) include the following: the use of both MODIS Aqua and Terra platforms to retrieve BRDF, which was made to simplify the quality control (QC) steps with more observations; the BRDF inversion method allowed negative coefficients, but the inversion was run once more without the negative coefficient to alleviate the issue since there is no non-negative least squares option in GEE; and also in order to make the framework widespread applicable instead of using station-measured incoming SW radiation, ERA5-Land 9-km incoming SW radiation was utilized. In addition, Sentinel-2 reflectance atmospheric correction was performed using the 6S model (Vermote*et al.* , 1997) through its

Python implementation (Py6S) instead of Sen2Cor.

In summary, the framework utilizes BRDF information from MODIS to account for differences in spectral albedo due to sensor-solar angular variability. This BRDF information is then downscaled to Sentinel-2 20-m resolution, and the high spatial resolution spectral albedo is converted to a broadband albedo using Li *et al.* (2018) conversion equations for Sentinel-2. The algorithm can be applied worldwide because it was implemented in GEE. The algorithm was run for both study area basins, and the mean snow and ice 20-m albedo within each HRU was extracted for DA. The station-measured albedo at Athabasca Ice AWS was utilized to evaluate the remotely sensed albedo estimates. This evaluation standard error was used as the satellite albedo measurement error for DA in both basins since the pixel that Peyto Main AWS falls within is not representative of snow and ice albedo due to infrastructure and bare soil contamination.

2.4. CRHM Hydrological Modelling

CRHM was used to predict streamflow in both basins without (CTRL) and with albedo data assimilation (DA). The CRHM configuration employed was similar to that of Pradhananga *et al.* (2022), with an updated firn and ice HRU designation from the two 2021-08-12 Sentinel-2 images in Figure 1. CRHM is a modular physically based hydrological model with a glacier energy and mass balance and routing modelling modules (Pomeroy*et al.* , 2022). The models were set up with 90 and 65 HRUs for AGRB and PGRB, respectively. The CTRL run used off-the-shelf constant albedos for ice (0.30) and firn (0.55). For spin-up purposes, the model was run from 2015-10-01 to 2021-09-30. Both models were forced with hourly station-measured air temperature, relative humidity, wind speed, incoming short- and long-wave radiation, and precipitation using the Athabasca Moraine and Peyto Main AWSs (Figure 1). These forcing variables were quality-controlled using the Fang *et al.* (2019) methodology. No calibration was performed in the CTRL or DA runs. Another difference in model configuration from Pradhananga and Pomeroy (2022) is that this study used a glacier and firn melt module employing a katabatic calculation of turbulent energy fluxes based on Grisogono and Oerlemans (2001) and tested in Peyto Glacier by Munro (2004) and Aubry-Wake *et al.* (2022b). This katabatic module represents the contribution of sub-daily glacier katabatic winds to the overall melt of ice and firn, advancing upon the less physically based configuration utilized by Pradhananga and Pomeroy (2022).

Snow albedo was simulated using the same algorithm employed in the Canadian Land Surface Scheme (CLASS) (Verseghy, 2012). The CRHM version used in this study has four other albedo algorithms capable of simulating snow albedo, including from observations and simply using a constant albedo. The model can calculate albedo using Gray and Landine (1987)'s method, which accounts for snow-covered area depletion in shallow snowpacks. The model can also simulate albedo utilizing Baker*et al.* (1990)'s method, which is based on a decay function that refreshes when snowfall occurs. Verseghy's algorithm evolves upon Barker's by accounting for differences between dry and wet snow and also taking into consideration daily mean temperatures, which is crucial in the context of heatwaves. Verseghy's algorithm was chosen to be used in this study given the widespread use of CLASS inside land surface and hydrology prediction systems in cold regions, e.g., in the Modélisation Environmentale Communautaire (MEC) - Surface and Hydrology (MESH) model (Pietroniro *et al.* , 2007; Wheater *et al.* , 2022). The chosen albedo algorithm feeds albedo information to the utilized energy balance snowmelt model SNOBAL (Marks *et al.* , 1998); therefore, it is expected that albedo assimilation will also have a large impact on snow depth and SWE.

2.5. Ensemble Kalman Filter Assimilation Framework

The DA period started in July 2017 when Sentinel-2 images became available at a higher revisit frequency, with the addition of Sentinel-2B. One individual Sentinel-2 scene was sufficient to cover each basin. Sentinel-2 images with less than 30% cloud cover were selected for albedo generation and as a DA date. If clouds or shadows completely covered an HRU, DA was not performed, but assimilation was executed for the other HRUs on the same date. DA was conducted using an EnKF method, following Clark *et al.* (2006) and Lv and Pomeroy (2020). EnKF was run with 20 ensemble members. Station-measured variables were perturbed with standard deviations displayed in Table 1. The standard deviation for less uncertain forcings (air temperature, relative humidity, incoming short- and long-wave radiation) was reduced to half of that used by Lv and Pomeroy (2020) since there is evidence that previously employed perturbation standard deviations were disproportionately large for these variables. For instance, Tang *et al.* (2023) have shown that hydrological modelling uncertainty due to temperature forcing is closer to 2 ºC instead of the commonly used 5 ºC. Wind speed and precipitation remain highly uncertain variables, and their standard deviations were kept the same as Lv and Pomeroy (2020).

Table 1: Station-measured forcings perturbed by prescribed standard deviations. The type of perturbation is also displayed.

Forcing	**Perturbation type**	**Standard deviation**
Air temperature [ºC]	Additive	2.50
Relative humidity [%]	Additive	5
Wind speed [m/s]	Additive	2
Incoming short-wave [W/m^2]	Multiplicative	0.15
Incoming long-wave [W/m^2]	Additive	25
Precipitation [mm]	Multiplicative	0.50

The implemented EnKF framework generates an optimal albedo estimate ($\hat{\alpha}$) between the CRHM modelled (α_m) and Sentinel-2 observed (α_o) albedo by weighing the modelling (σ_m^2) and measurement error variance (σ_o^2) using the Kalman gain (K),

$$\hat{\alpha} = (1 - K)\,\alpha_m + K\alpha_o \qquad (1)$$

$$K = \sigma_m^2/(\sigma_m^2 + \sigma_o^2) \qquad (2)$$

Modelling error (σ_m^2) was determined by the departure from the mean of the 20 modelled albedos, and measurement error (σ_o^2) was defined by utilizing the standard error from Sentinel-2 albedo evaluation with Athabasca Ice AWS. Snow depth, SWE, snowpack cold content, water in the snowpack, firn and ice total water equivalents were also updated proportionally to K. Other related variables were updated to maintain physical coherence when updating the latter state variables. For example, snow density was updated based on the new snow depth and SWE states. The above DA process was repeated the same number of times as of available Sentinel-2 albedo estimates for each basin until the whole period was covered. CRHM streamflow simulations were continued for an extra two days with old model states into the new assimilation interval. This procedure was performed to cover the first two days in which streamflow calculated with the new states was still being routed through the basin. The period of two days was chosen because it covers the time of concentration for both basins.

2.6. Streamflow Evaluation

Model performance with and without DA was only assessed in the last four WYs because they had a complete Sentinel-2 albedo time series. These years also encompassed very contrasting environmental conditions: a heavily wildfire soot-impacted WY (2018); a mildly soot-impacted WY (2019) from algae feeding from 2017 and 2018 soot; a normal WY (2020); and a WY impacted by heatwaves (2021). Streamflow prediction performance was estimated by the Nash-Sutcliffe Efficiency (NSE) coefficient (Nash and Sutcliffe, 1970), bias, RMSE, and the KGE coefficient (Gupta *et al.* , 2009). The evaluation was made considering the entire four WY periods and on a WY basis. It is worth noting that streamflow in these two glacierized basins is limited to the spring and summer seasons (May to Sept.).

3. Results

3.1. Remotely Sensed Albedo Evaluation

Remotely sensed albedo presented satisfactory results for the Athabasca Ice AWS evaluation. Twenty-eight matching observations were available for evaluation. Albedo correlation was 0.96, bias was 0.026, RMSE was 0.060, and the regression model standard error (σ_o) was 0.046 (Figure 2). It was important to calculate σ as this metric determines the remote sensing measurement error necessary for DA. In summary, snow albedos were less accurate than ice albedos. Snow albedos had a higher spread and positive bias, whereas ice albedo errors were more evenly distributed around the 1:1 line. These results were similar to those previously found in the literature with r, bias, and RMSE values between 0.82 and 0.88 (Shuai *et al.* , 2011; Bertoncini*et al.* , 2022), -0.029 and 0.019, and 0.025 and 0.043 (Shuai*et al.* , 2011; Wang *et al.* , 2016; Li *et al.* , 2018; Bertoncini *et al.* , 2022), respectively.

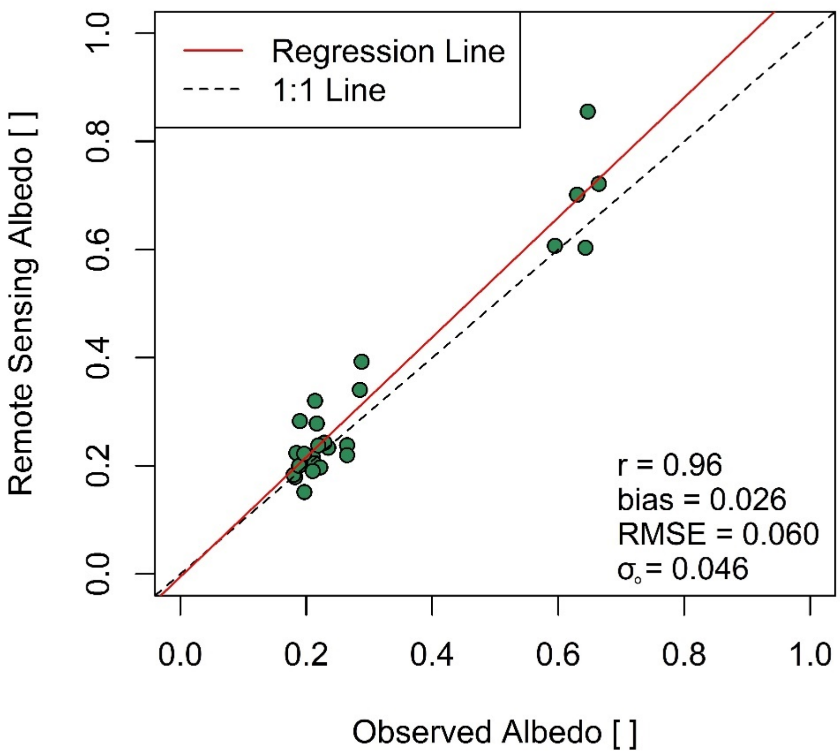

Figure 2: Remotely sensed albedo evaluation for Athabasca Ice AWS.

Figure 3 shows both basins' mid-summer remotely sensed snow and ice albedo maps. These maps demonstrate the vast spatial variability of intra-HRU and -basin snow and ice albedos. Such spatial variabilities cannot be captured by modelling in scales smaller than its HRU units. Although the intra-HRU albedo variability was averaged out before DA was performed, the collective variations caused by wildfires and heatwaves can generate different integrated responses. This heterogeneity suggests that the remotely sensed albedos can contribute new information to a cold regions DA framework. Intra-basin snow and ice albedo variability is also observed in both basins. For example, in AGRB, there is a clear distinction between lower glacier ice albedos and the higher albedos from the Columbia Icefield. The transition from snow to firn albedos is also evident in PGRB. This date also exhibits an area in which albedo was not retrieved for the most terminal glacier HRU in PGRB. Masked albedo values in Figure 3 can occur if clouds and shadows obstruct the area or if the coarse resolution BRDF retrieval is unable to generate enough observations for a particular landcover class. DA was not performed when there were no snow and ice 20-m albedo pixels inside an HRU, and the modelling continued with its old state variables. Note that there were 68 and 33 dates with available remotely sensed albedo estimates for assimilation in AGRB and PGRB, respectively.

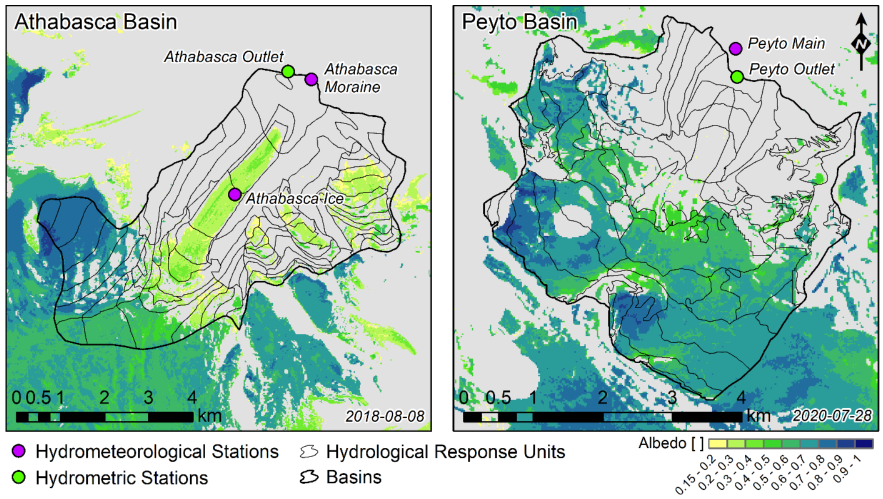

Figure 3: Remotely sensed snow and ice albedos for both basins during mid-summer conditions. Light grey corresponds to masked areas due to snow- and ice-free pixels, obstruction by clouds and shadows, or if the BRDF retrieval was not possible for that landcover class.

3.2. Albedo DA Streamflow Evaluation

DA and CTRL streamflow evaluation metrics had accurate results for most analyzed years. In the heavily wildfire-impacted year of 2018, DA outperformed CTRL for both basins. The KGE difference between DA and CTRL was 0.18 and 0.20 for AGRB and PGRB, respectively. In 2019 (soot algae growth) and 2020 (normal year), DA was only beneficial for PGRB. In 2021, the year affected by heatwaves and a few light late summer wildfires, DA did not improve streamflow predictions for either basins, indicating that other mechanisms might have influenced streamflow predictions during heatwave conditions or that the operation of the albedo algorithm in CRHM could not be improved upon by assimilating observations. The four-year overall evaluation revealed that albedo DA substantially benefited streamflow predictions in PGRB (KGE improvement of 0.12), but only a slight advantage was found for streamflow predictions in AGRB (KGE improvement of 0.02) (Table 2). The four-year overall evaluation NSEs for AGRB (0.74) and PGRB (0.78) were above the mean of maximum values (0.64) found in 20 studies that predicted streamflow with the CRHM model (Pomeroy *et al.* , 2022).

Table 2: Streamflow evaluation metrics for AGRB and PGRB. Metrics were calculated for the combined four melt seasons and each melt season individually (May 1 to Sept. 30), since streamflow rarely occurs outside that period.

Athabasca Glacier Research Basin (AGRB)

Period	**NSE DA**	**NSE CTRL**
2018	0.63	0.43
2019	0.54	0.67
2020	0.83	0.82
2021	0.83	0.86
4-year	0.74	0.73
Peyto Glacier Research Basin (PGRB)	**Peyto Glacier Research Basin (PGRB)**	**Peyto Glacier Research I**
Period	**NSE DA**	**NSE CTRL**
2018	0.82	0.64

2019	0.68	0.22
2020	0.85	0.56
2021	0.71	0.77
4-year	0.78	0.63

Improvements in streamflow predictions occurred because DA decreased streamflow compared to the CTRL run, reducing its positive bias. This situation was observed particularly during the wildfires of 2018 for both basins, but also in 2019, 2020, and the four-year period for PGRB. The overall decrease in positive bias by DA is noticeable in Figure 4, in which the CRTL streamflow (red) appears distinctly larger than the DA streamflow (blue) in years that improvement was observed, except for 2021 in PGRB when CTRL streamflow was higher than DA. The reason for the overall DA decrease in streamflow predictions will be further discussed in section 5.4.3.

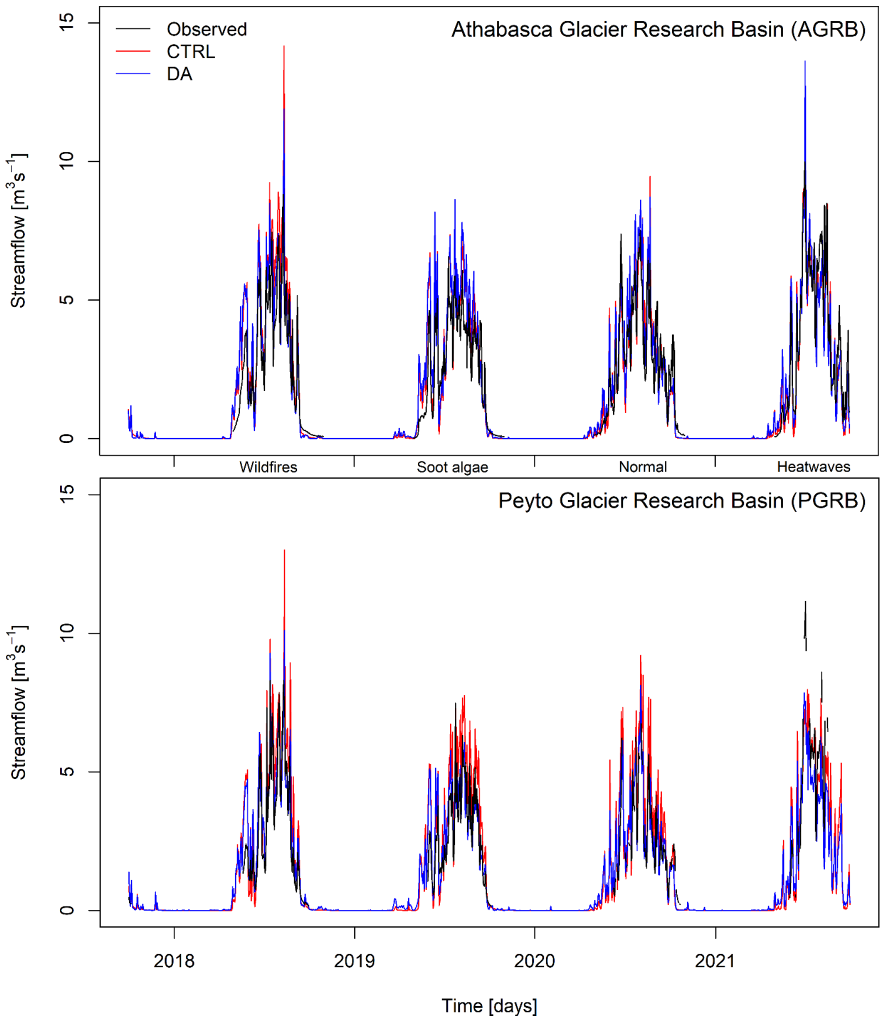

Figure 4: AGRB (top) and PGRB (bottom) observed and simulated DA and CTRL streamflows for the four analyzed WYs.

3.3. Albedo and SWE Updating with DA

As stated in section 5.4.2, satellite albedo DA improvements were observed in years when DA streamflow predictions were lower than CTRL and bias was positive. The benefit of satellite DA was caused by a decrease in modelled glacier albedo combined with an increase in snowcover in spring and summer (Figures 5, 6, and Table 2). This mechanism occurs because the associated melt decreases considerably while snowcover covers glacier ice, considering the relatively high albedo snow generates less meltwater than relatively low albedo ice for the same shortwave insolation fluxes. The DA streamflow used for evaluation was the mean of all 20 ensembles. This mean is lower if more ensembles have prolonged spring and summer snowcover over ice. Since the benefits of DA stem from a decrease in streamflow, snowcover over ice has a larger influence on melt than the decrease in albedo introduced by DA. In AGRB, the ice albedo decrease introduced by DA was larger than in PGRB. At the same time, the DA snowcover over ice was smaller in AGRB (Figures 5 and 6). The integrated response was that AGRB streamflow was less sensitive to DA than in PGRB. These results indicate that the benefit of satellite albedo DA stems not only from the albedo itself, but also from associated changes in other model states and glacier configuration.

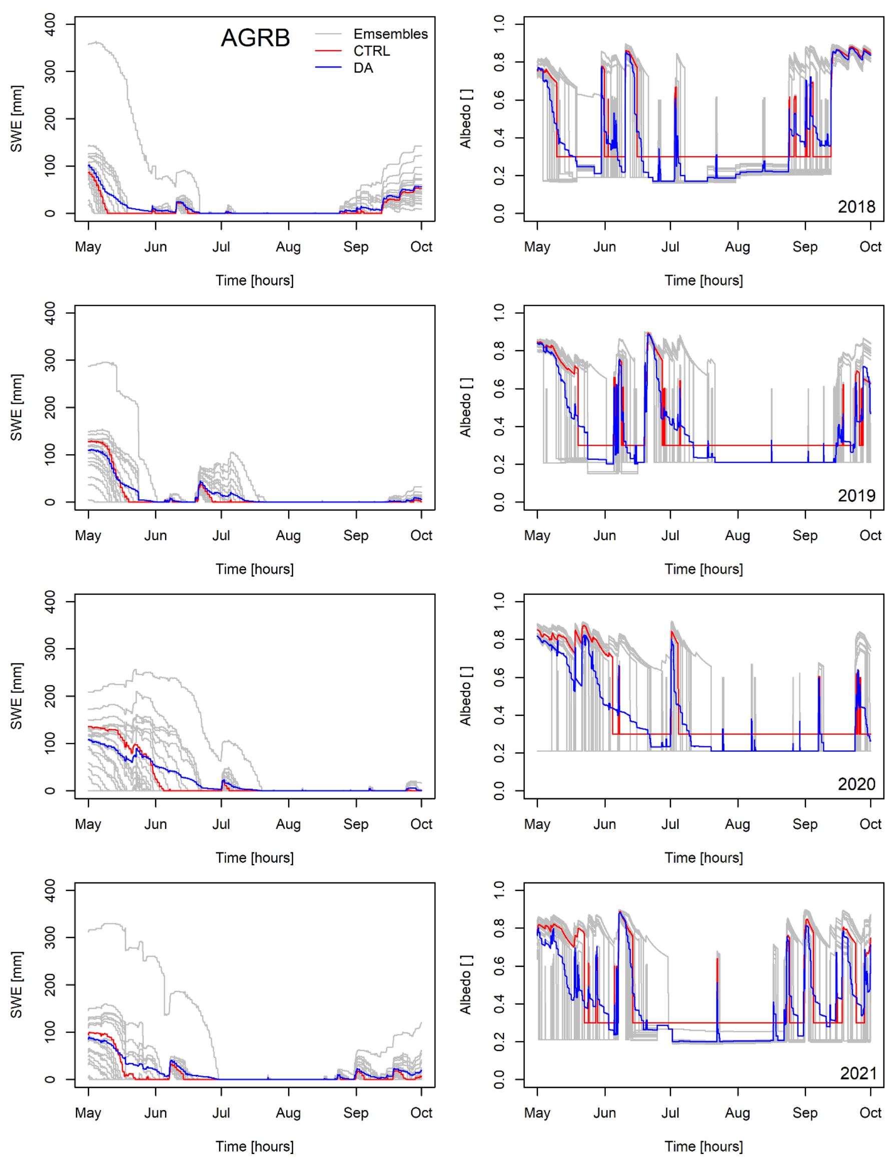

Figure 5: AGRB SWE and albedo DA mean, control, and ensembles for the four melt seasons at the highlighted glacier ice HRU in Figure 1.

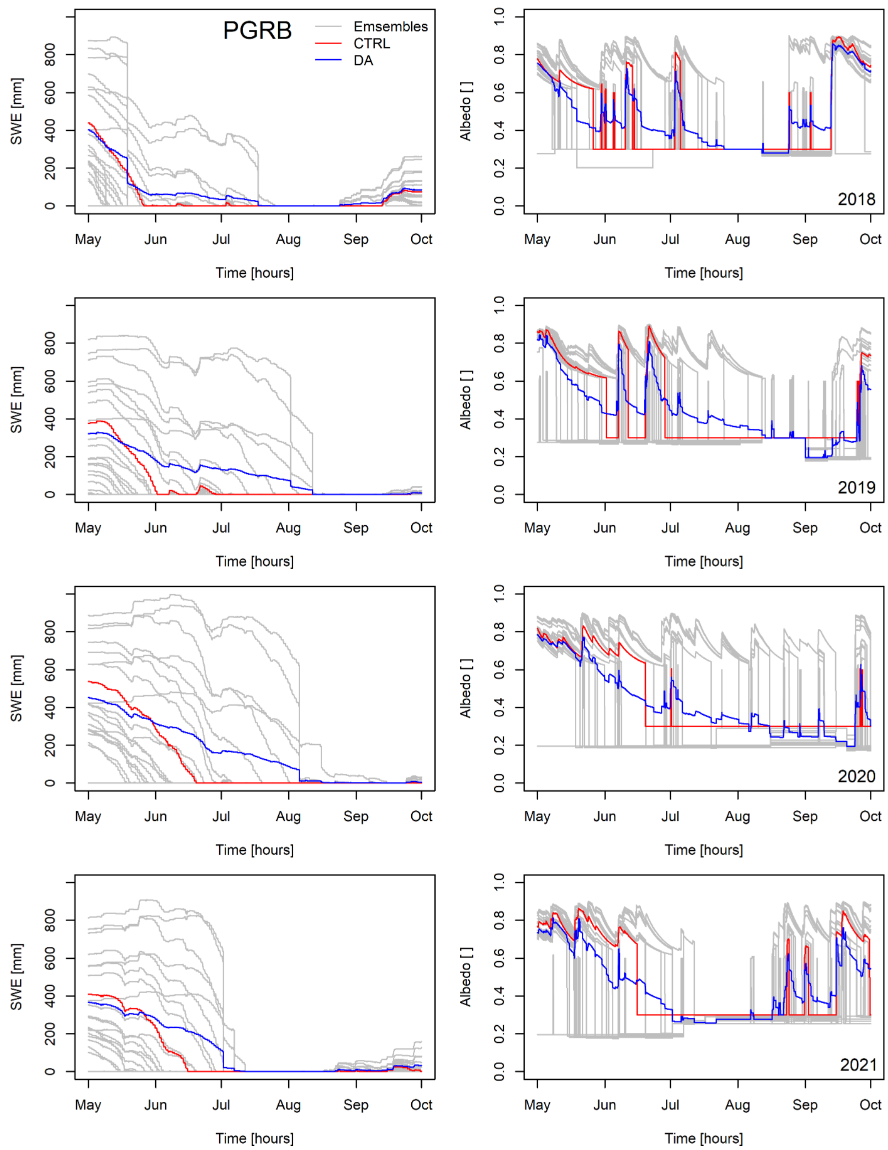

Figure 6: PGRB SWE and albedo DA mean, control, and ensembles for the four melt seasons at the highlighted glacier ice HRU in Figure 1.

3.4. Albedo DA Differences Between Snow and Ice HRUs

A prolonged spring and summer snowcover over glacier ice is not the only cause of decreased streamflow in these basins. Because streamflow at the outlet of glacierized basins is an integrated response of mainly snow, firn, and ice melt, the melt at higher elevation snow and firn HRUs is also relevant to the overall streamflow contribution. Figures 7 and 8 show the modelled albedo during wildfire (2018) and heatwave (2021) conditions for snow and glacier ice HRUs in AGRB and PGRB, respectively. Figure 7 illustrates that although AGRB DA albedo is lower for glacier ice during wildfires and heatwaves, it is higher in snow-dominated regions. The larger albedo in AGRB snow compensates for the smaller albedo in glacier ice in years (e.g., 2018) when DA improved streamflow predictions. Figure 8 shows that albedos were commonly smaller with DA in PGRB snow, but in ice, they were only persistently lower than CTRL during heatwaves. A larger DA PGRB ice albedo explains why streamflow prediction improvements are better for this basin since the positive bias in CTRL is decreased even further. During the 2021 heatwaves, DA could not substantially improve streamflow predictions in either basin. However, AGRB DA was closer to observed streamflows when compared to PGRB. This difference can be explained by the longer persistence of DA snowcover over ice in PGRB than AGRB. DA snow albedo in PGRB was closer to CTRL, thus contributing to an even smaller streamflow for that year (Figure 8). The results suggest that the albedo decay algorithm was capable of simulating albedo in a heatwave, but could not predict the lower albedos due to soot from wildfires.

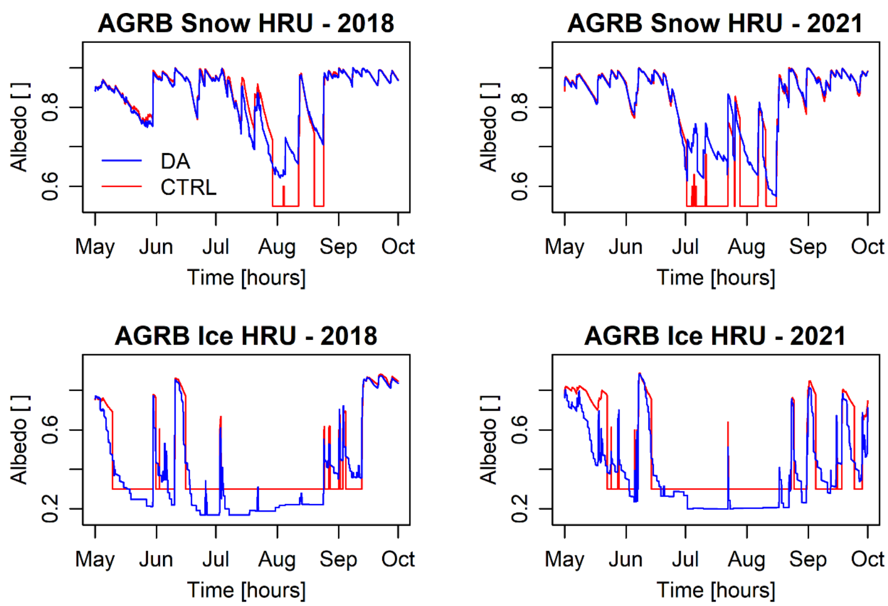

Figure 7: AGRB spring and summer DA and CTRL albedos at the snow and glacier ice HRUs highlighted in Figure 1. The 2018 and 2021 years are shown to represent wildfire and heatwave conditions, respectively.

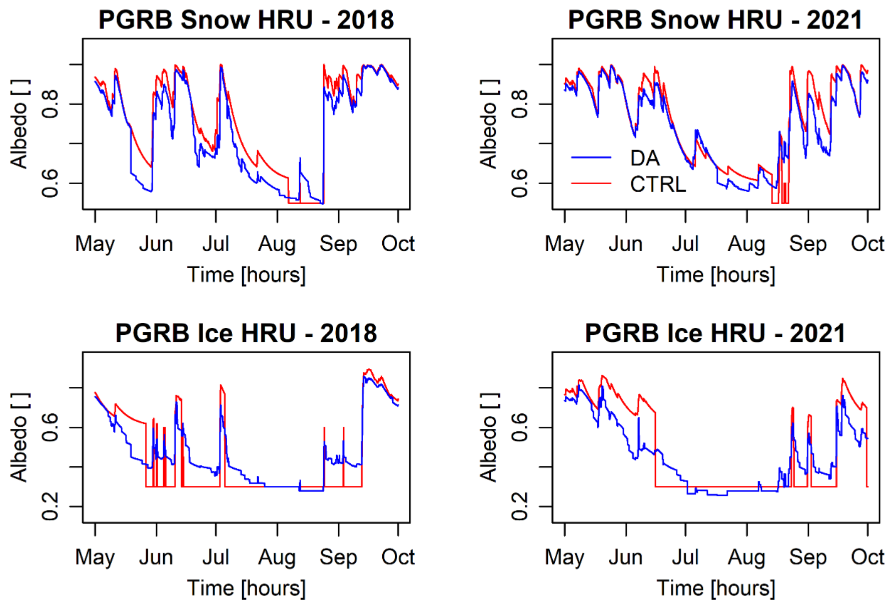

Figure 8: PGRB spring and summer DA and CTRL albedos at the snow and glacier ice HRUs highlighted in Figure 1. The 2018 and 2021 years are shown to represent wildfire and heatwave conditions, respectively.

4. Discussions

4.1. Albedo DA During Wildfire and Heatwave Conditions

The results presented in the previous sections have demonstrated that albedo DA can improve streamflow simulations during wildfires but not during heatwaves. The streamflow improvement response to albedo DA in the soot-feeding algae year was only considerable in PGRB. These results reveal somewhat contrasting processes happening in different zones of these basins. Over glacier ice, DA decreased albedo considerably for AGRB due to wildfire soot deposition, a process that was expected and confirmed in previous studies (Aubry-Wake *et al.* , 2022a; Bertoncini *et al.* , 2022). In PGRB, the decrease in ice albedo due to DA was not as pronounced because of prolonged spring and summer snowcover over ice. SWE is another state that is updated proportionally to albedo. Because these states are the mean of 20 ensembles, the likelihood of all ensembles converging in the absence of a snowpack becomes lower when several ensembles present elevated SWE values. Figures 5 and 6 show that the SWE ensemble spread in PGRB was wider than in AGRB, contributing to a shorter period of exposed ice in PGRB. This mechanism could have been caused by deeper snowpacks observed in terminal sections of PGRB and more frequent spring and summer snowfall events. The effect of prolonged snowcover when compared to control simulations in snow DA has been reported before, usually leading to snow depletion simulations closer to observations (Smyth *et al.* , 2020; Alonso-González *et al.* , 2022). It is worth noting that once the snow is depleted and firn and ice are exposed, temperature-driven albedo decrease ceases. This mechanism should be captured by the albedo decay algorithm that uses constant albedo values for exposed firn and ice. The latter can potentially explain why streamflow predictions were not sensitive to albedo DA during the heatwave year.

Unlike ice, snow has a different response to albedo DA. Albedo DA has shown to be larger than modelled by CTRL in AGRB high-elevation snow-dominated regions. The introduction of remotely sensed albedo through DA has revealed that snow was not completely melted in the AGRB high-elevation HRU examples displayed in Figure 7, i.e., albedo did not reach the 0.55 firn value. The low CTRL snow albedos can be a limitation of albedo algorithms based on decay functions, such as the one used hereby, which were developed for seasonal snowpacks at much lower elevations. A comparison of three empirical models with a full physically based model (closer to observations) has shown that empirical decay albedo models, indeed, underestimate snow albedo (Gardner and Sharp, 2010). On the other hand, DA snow albedo is often below CTRL in PGRB, but rarely reaches the firn value of 0.55 (Figure 8). This result suggests that snow-dominated PGRB surfaces would have a lower DA albedo than CTRL, since they are more heterogeneous due to greater firn and ice exposure than in AGRB. CTRL seems to miss processes well described at lower elevations but not at glacier accumulation zones in both basins. This finding calls for a better representation of glaciological albedo processes capable of accounting for the peculiarities of localized effects (Marshall and Miller, 2020).

This study tested two main assumptions by introducing remotely sensed albedo in a cold regions DA framework. First, soot deposition would decrease snow and ice albedo during extreme wildfire activity, such as in 2018. This assumption was confirmed by previous studies (Aubry-Wake*et al.* , 2022a; Bertoncini *et al.* , 2022) and hereby for ice in AGRB and snow in PGRB. A greater albedo in the AGRB snow HRU example can be explained by the larger elevation range observed between snow and ice regions in AGRB (Pradhananga and Pomeroy, 2022). This larger elevation range creates a scenario in which snow-covered plateaux are at elevations more prone to new snowfall, suppressing the effect of soot deposition over snow at a faster pace. Rapid recovery from soot deposition over high-elevation snow in AGRB has been previously described in Bertoncini *et al.* (2022). Second, heatwaves would accelerate melt and expose ice or firn unseasonally. This process does not seem to substantially affect AGRB ice since exposure in 2021 is similar to other years. However, albedo is lower for snow during heatwaves when compared to wildfire years. Substantial snowmelt and decreased albedo in glacier snow due to extended periods of above-average temperature have been reported before in Greenland (Box*et al.* , 2022) and the Austrian Alps (Koboltschnig *et al.* , 2009). This mechanism suggests that heatwaves have a greater influence on high-elevation snow-covered plateaux albedo decreases than does wildfire soot in AGRB. On the other hand, there is a larger sensitivity to wildfires than heatwaves for PGRB snow, perhaps because of more firn and ice exposure than in AGRB. PGRB ice shows greater albedo decrease during heatwaves due to longer ice exposure. In addition, the albedo algorithm is expected to be more robust during heatwaves than wildfires because it considers daily mean temperatures, limiting most albedo DA benefits to wildfire years.

4.2. Implications for Streamflow Prediction in a Changing Climate

Unprecedented wildfires and heatwaves are expected to increase with climate change (Jolly *et al.* , 2015; Kirchmeier-Young *et al.* , 2019; Al-Yaari *et al.* , 2023; Parisien *et al.* , 2023) and, hence, are likely to affect glacier contribution to streamflow. Although this is a somewhat intuitive assumption, this study has demonstrated inter- and intra-basin peculiarities in how the effects of wildfires and heatwaves will contribute to snow and ice melt. The findings show that wildfires and heatwaves can decrease glacier ice albedo, but the period that ice is covered by snow is the primary governing factor controlling ice melt. Likewise, the amount of summer precipitation falling as snowfall is another factor governing albedo dynamics in snow-dominated regions. This mechanism creates a scenario where the elevation difference from the terminal glacier to high-elevation snow plateaus dictates whether these basins would be affected by either wildfires or heatwaves. For instance, in AGRB where this elevation difference was higher than in PGRB, DA generated an increase in snow albedo. This finding alone reveals something that would not be possible using modelling alone; remotely sensed albedos were needed in a DA modelling framework to understand this process in a virtually inaccessible region. There lies the power of observational tools in aiding hydrological models beyond the conditions in which they were developed.

There are many implications of remotely sensed albedo DA for streamflow predictions under climate change. The most important one is that this study showed that even though DA was not beneficial for streamflow prediction during heatwaves, it was beneficial in the overall four-year evaluation in PGRB and favourable during wildfires and similar to CTRL in other years in AGRB. From this perspective, remotely sensed albedo DA is recommended under unprecedented hydrological extremes imposed by climate change; however, caution should be taken when interpreting albedo DA results during heatwaves. The latter calls for further investigation into other processes that might have contributed to albedo DA degradation of streamflow predictions under heatwaves beyond what has been discussed here. Remotely sensed albedo DA can also better inform hydrological modelling during wildfires and heatwaves. For instance, events of decreased albedo can happen in the future in high-elevation snow-dominated regions but be buffered subsequently by fresh snowfall, which can only be confirmed with certainty via remotely sensed albedos since precipitation measurements are usually taken at much lower rainfall-dominated elevations. Users of hydrological predictions can then understand *de facto* whether these extreme events will affect downstream streamflows.

4.3. Uncertainty within DA Modelling Framework

The DA modelling framework has worked satisfactorily in most simulated years; however, a few factors contributed to the uncertainty in modelling streamflow and other model states. First, although snow and ice remotely sensed albedo estimates were satisfactory here and elsewhere (Wang *et al.* , 2016; Li *et al.* , 2018; Bertoncini*et al.* , 2022), there is still a 5% uncertainty (σ_o = 0.046) in albedo estimation. This 5% uncertainty cannot be neglected in glacier ice albedo values. Therefore, even if modelling uncertainty is larger than 5%, this value would be, on average, the smallest uncertainty possible of an optimal albedo estimate for a particular assimilation date. Second, assimilation frequency can contribute to the influence of DA in modelling albedo and other states. AGRB (68 estimates) had more than double the number of assimilation dates of PGRB (33 estimates). The lower number of assimilation dates in PGRB could have contributed to longer periods of snowcover over ice, since albedo correction from a new remotely sensed update would take longer to occur. Finally, uncertainty in hydrological modelling can also affect streamflow prediction within a DA framework. This study presented DA NSE values of 0.74 and 0.78 for AGRB and PGRB, respectively. These NSE values are higher than the mean of maximum values (0.64) found in 20 studies that conducted uncalibrated streamflow predictions using the CRHM model (Pomeroy *et al.* , 2022). Nonetheless, these NSE values are not perfect, i.e., equal to 1, representing that there are still uncertainties in streamflow prediction that can be attributed to model structure, forcing errors, parameter errors, algorithm deficiencies, and uncertainty caused by the DA EnKF implementation.

5. Conclusions

This research implemented and tested a remotely sensed albedo DA framework to predict streamflow in two highly glacierized Canadian Rockies's basins during environmental conditions ranging from normal, wildfire, and heatwave dominated. Glacier ice remotely sensed albedos presented satisfactory evaluation results (r = 0.96, bias = 0.026, RMSE = 0.060, and σ_o = 0.046) that were needed for assimilation. Albedo DA improved streamflow predictions in the heavily wildfire-impacted year of 2018 for both basins − a KGE improvement of 0.18 and 0.20 for AGRB and PGRB, respectively. DA in PGRB was beneficial for all years but 2021. In the soot-feeding algae year, streamflow improvement due to albedo DA was only considerable in PGRB. DA substantially enhanced overall four-year streamflow prediction in PGRB but just slightly in AGRB. DA's streamflow prediction improvements were caused by a balance between changes in albedo of high-elevation snow and glacier ice. In AGRB, snow albedo was increased by DA due to frequent summer snowfall events that buffered the streamflow generated from decreased glacier ice albedo in lower elevations. In PGRB, snow albedo was decreased by DA, especially during wildfires. However, glacier ice DA albedo was only decreased during short periods of ice exposure caused by a prolonged spring and summer snowpack. The latter mechanism results from several ensembles generating elevated SWE values during spring and summer in PGRB glacier ice. These findings reveal that wildfires and heatwaves are capable of decreasing glacier ice albedo, but the resultant melt contribution to streamflow within a DA framework will depend on snowpack albedo and SWE dynamics.

The cloud-computing remotely sensed snow and ice albedo retrieval framework developed in this study could generate results with comparable accuracy to previous studies, while providing global reproducibility at high spatial and temporal resolutions. Before this study, albedo in snow-dominated glacier accumulation zones was based solely on albedo modelling developed at relatively lower elevations. This albedo representation could not account for the rapid recovery of albedo with fresh snowfall during wildfire and heatwave seasons. This finding was only possible utilizing high-resolution remotely sensed albedo estimates that could reach virtually inaccessible regions. The assimilation of these remotely sensed albedo estimates into the physically based CRHM model improved streamflow predictions for most of the analyzed years. Moreover, using albedo DA revealed contrasting processes happening in poorly observed glacier zones that resulted in different streamflow responses to wildfires and heatwaves. Considering that the environmental conditions observed during the study are expected to increase in a future of climate change, it can be advantageous to use remotely sensed high-resolution snow and ice albedo DA continuously for better streamflow predictions in glacierized basins during wildfires and heatwaves. This study's findings also indicate that the response of glacierized basin streamflow to wildfires and heatwaves is not always as expected due to the interplay of different factors such as fresh snowfall, soot deposition, and unseasonal melt with the albedo algorithm. Using observational tools such as DA can help narrow water managers' uncertainty when making decisions based on hydrological predictions under a warmer and more wildfire prone future.

Acknowledgements

We wish to thank NASA for the MODIS data and the European Space Agency (ESA) for the Sentinel-2 and ERA5-Land data used to estimate remotely sensed high-resolution albedos. We also acknowledge the support of the GEE platform for hosting the above data and providing cloud-computing resources, and the developers of the 6S atmospheric correction model and its Python implementation (Py6S). The help from Xing Fang to QC meteorological forcings and to set up the CRHM model is much appreciated. We thank Caroline Aubry-Wake and Dhiraj Pradhananga for the discussions about glacio-hydrological modelling and the many Centre for Hydrology field technicians who contributed to maintaining the AWS. We also would like to acknowledge the permission of Parks Canada for allowing our research to take place in the Banff and Jasper National Parks and Pursuit for assistance in logistics on Athabasca Glacier.

6. References

Al-Yaari A, Zhao Y, Cheruy F, Thiery W. 2023. Heatwave Characteristics in the Recent Climate and at Different Global Warming Levels: A Multimodel Analysis at the Global Scale. *Earth's Future* **11** (9): 1–18 DOI: 10.1029/2022EF003301

Alfieri L, Burek P, Dutra E, Krzeminski B, Muraro D, Thielen J, Pappenberger F. 2013. GloFAS-global ensemble streamflow forecasting and flood early warning. *Hydrology and Earth System Sciences* **17** (3): 1161–1175 DOI: 10.5194/hess-17-1161-2013

Alonso-González E, Aalstad K, Baba MW, Revuelto J, López-Moreno JI, Fiddes J, Essery R, Gascoin S. 2022. The Multiple Snow Data Assimilation System (MuSA v1.0). *Geoscientific Model Development* **15**(24): 9127–9155 DOI: 10.5194/gmd-15-9127-2022

Andreadis KM, Lettenmaier DP. 2006. Assimilating remotely sensed snow observations into a macroscale hydrology model. *Advances in Water Resources* **29** (6): 872–886 DOI: 10.1016/j.advwatres.2005.08.004

Aubry-Wake C, Bertoncini A, Pomeroy JW. 2022a. Fire and Ice: The Impact of Wildfire-Affected Albedo and Irradiance on Glacier Melt. *Earth's Future* **10** (4) DOI: 10.1029/2022EF002685

Aubry-Wake C, Pradhananga D, Pomeroy JW. 2022b. Hydrological process controls on streamflow variability in a glacierized headwater basin. *Hydrological Processes* **36** (10) DOI: 10.1002/hyp.14731

Baars H, Ansmann A, Ohneiser K, Haarig M, Engelmann R, Althausen D, Hanssen I, Gausa M, Pietruczuk A, Szkop A, et al. 2019. The unprecedented 2017-2018 stratospheric smoke event: Decay phase and aerosol properties observed with the EARLINET. *Atmospheric Chemistry and Physics* **19** (23): 15183–15198 DOI: 10.5194/acp-19-15183-2019

Baker DG, Ruschy DL, Wall DB. 1990. The Albedo Decay of Prairie Snows. *Journal of Applied Meteorology* **29** (2): 179–187 DOI: 10.1175/1520-0450(1990)029<0179:TADOPS>2.0.CO;2

Bergström S, Lindström G. 2015. Interpretation of runoff processes in hydrological modelling-experience from the HBV approach. *Hydrological Processes* **29** (16): 3535–3545 DOI: 10.1002/hyp.10510

Bertoncini A, Aubry-Wake C, Pomeroy JW. 2022. Large-area high spatial resolution albedo retrievals from remote sensing for use in assessing the impact of wildfire soot deposition on high mountain snow and ice melt. *Remote Sensing of Environment* **278** (June 2021) DOI: 10.1016/j.rse.2022.113101

Beven K. 2012. *Rainfall-Runoff Modelling: The Primer* . Wiley-Blackwell: Lancaster, UK.

Blöschl G, Hall J, Viglione A, Perdigão RAP, Parajka J, Merz B, Lun D, Arheimer B, Aronica GT, Bilibashi A, et al. 2019. Changing climate both increases and decreases European river floods. *Nature***573** (7772): 108–111 DOI: 10.1038/s41586-019-1495-6

Box JE, Wehrlé A, van As D, Fausto RS, Kjeldsen KK, Dachauer A, Ahlstrøm AP, Picard G. 2022. Greenland Ice Sheet Rainfall, Heat and Albedo Feedback Impacts From the Mid-August 2021 Atmospheric River.*Geophysical Research Letters* **49** (11) DOI: 10.1029/2021GL097356

Clark MP, Rupp DE, Woods RA, Zheng X, Ibbitt RP, Slater AG, Schmidt J, Uddstrom MJ. 2008. Hydrological data assimilation with the ensemble Kalman filter: Use of streamflow observations to update states in a distributed hydrological model. *Advances in Water Resources***31** (10): 1309–1324 DOI: 10.1016/j.advwatres.2008.06.005

Clark MP, Slater AG, Barrett AP, Hay LE, McCabe GJ, Rajagopalan B, Leavesley GH. 2006. Assimilation of snow covered area information into hydrologic and land-surface models. *Advances in Water Resources***29** (8): 1209–1221 DOI: 10.1016/j.advwatres.2005.10.001

Dumont M, Durand Y, Arnaud Y, Six D. 2012. Variational assimilation of albedo in a snowpack model and reconstruction of the spatial mass-balance distribution of an alpine glacier. *Journal of Glaciology* **58** (207): 151–164 DOI: 10.3189/2012JoG11J163

Esser M, Ankley P, Aubry-Wake C, Xie Y, Baulch H, Hoggarth C, Hecker M, Hollert H, Giesy JP, Pomeroy JW, et al. (accepted manuscript) A Preliminary Investigation of Microbial Communities on the Athabasca Glacier Within Deposited Organic Matter. *Environmental Science: Advances*

Evensen G. 1994. Sequential data assimilation with a nonlinear quasi-geostrophic model using Monte Carlo methods to forecast error statistics. *Journal of Geophysical Research* **99** (C5) DOI: 10.1029/94jc00572

Fang X, Pomeroy JW. 2007. Snowmelt runoff sensitivity analysis to drought on the Canadian prairies. *Hydrological Processes***21** (19): 2594–2609 DOI: 10.1002/hyp.6796

Fang X, Pomeroy JW, Debeer CM, Harder P, Siemens E. 2019. Hydrometeorological data from Marmot Creek Research Basin, Canadian Rockies. *Earth System Science Data* **11** (2): 455–471 DOI: 10.5194/essd-11-455-2019

Flanner MG, Zender CS, Randerson JT, Rasch PJ. 2007. Present-day climate forcing and response from black carbon in snow. *Journal of Geophysical Research Atmospheres* **112** (11): 1–17 DOI: 10.1029/2006JD008003

Gardner AS, Sharp MJ. 2010. A review of snow and ice albedo and the development of a new physically based broadband albedo parameterization.*Journal of Geophysical Research: Earth Surface* **115** (1): 1–15 DOI: 10.1029/2009JF001444

Gray DM, Landine PG. 1987. Albedo model for shallow prairie snow covers.*Canadian Journal of Earth Sciences* **24** (9): 1760–1768 DOI: 10.1139/e87-168

Greuell W, Reijmer CH, Oerlemans J. 2002. Narrowband-to-broadband albedo conversion for glacier ice and snow based on aircraft and near-surface measurements. *Remote Sensing of Environment* **82** (1): 48–63 DOI: 10.1016/S0034-4257(02)00024-X

Grisogono B, Oerlemans J. 2001. A theory for the estimation of surface fluxes in simple katabatic flows. *Quarterly Journal of the Royal Meteorological Society* **127** (578): 2725–2739 DOI: 10.1002/qj.49712757811

Gupta H V., Kling H, Yilmaz KK, Martinez GF. 2009. Decomposition of the mean squared error and NSE performance criteria: Implications for improving hydrological modelling. *Journal of Hydrology***377** (1–2): 80–91 DOI: 10.1016/j.jhydrol.2009.08.003

Hamlet AF, Lettenmaier DP. 2007. Effects of 20th century warming and climate variability on flood risk in the western U.S. *Water Resources Research* **43** (6): 1–17 DOI: 10.1029/2006WR005099

Hamman JJ, Nijssen B, Bohn TJ, Gergel DR, Mao Y. 2018. The variable infiltration capacity model version 5 (VIC-5): Infrastructure improvements for new applications and reproducibility. *Geoscientific Model Development* **11** (8): 3481–3496 DOI: 10.5194/gmd-11-3481-2018

Huang C, Newman AJ, Clark MP, Wood AW, Zheng X. 2017. Evaluation of snow data assimilation using the ensemble Kalman filter for seasonal streamflow prediction in the western United States. *Hydrology and Earth System Sciences* **21** (1): 635–650 DOI: 10.5194/hess-21-635-2017

Jolly WM, Cochrane MA, Freeborn PH, Holden ZA, Brown TJ, Williamson GJ, Bowman DMJS. 2015. Climate-induced variations in global wildfire danger from 1979 to 2013. *Nature Communications* **6** (May): 1–11 DOI: 10.1038/ncomms8537

Kirchmeier-Young MC, Gillett NP, Zwiers FW, Cannon AJ, Anslow FS. 2019. Attribution of the Influence of Human-Induced Climate Change on an Extreme Fire Season. *Earth's Future* **7** (1): 2–10 DOI: 10.1029/2018EF001050

Koboltschnig GR, Schöner W, Holzmann H, Zappa M. 2009. Glaciermelt of a small basin contributing to runoff under the extreme climate conditions in the summer of 2003. *Hydrological Processes* **23** (7): 1010–1018 DOI: 10.1002/hyp.7203

Kreibich H, Van Loon AF, Schröter K, Ward PJ, Mazzoleni M, Sairam N, Abeshu GW, Agafonova S, AghaKouchak A, Aksoy H, et al. 2022. The challenge of unprecedented floods and droughts in risk management. *Nature* **608** (7921): 80–86 DOI: 10.1038/s41586-022-04917-5

Krysanova V, Vetter T, Eisner S, Huang S, Pechlivanidis I, Strauch M, Gelfan A, Kumar R, Aich V, Arheimer B, et al. 2017. Intercomparison of regional-scale hydrological models and climate change impacts projected for 12 large river basins worldwide - A synthesis. *Environmental Research Letters* **12** (10) DOI: 10.1088/1748-9326/aa8359

Li X, Gao F, Wang J, Strahler A. 2001. A priori knowledge accumulation and its application to linear BRDF model inversion. *Journal of Geophysical Research: Atmospheres* **106** (D11): 11925–11935 DOI: 10.1029/2000JD900639

Li Z, Erb A, Sun Q, Liu Y, Shuai Y, Wang Z, Boucher P, Schaaf C. 2018. Preliminary assessment of 20-m surface albedo retrievals from sentinel-2A surface reflectance and MODIS/VIIRS surface anisotropy measures. *Remote Sensing of Environment* **217** (October 2017): 352–365 DOI: 10.1016/j.rse.2018.08.025

Liang S. 2000. Narrowband to broadband conversions of land surface albedo I: Algorithms. Remote Sensing of Environment, 76(2), 213-238. *Remote Sensing of Environment* **76** (2): 213–238 DOI: 10.1016/S0034-4257(00)00205-4

Lin H, Mo R, Vitart F. 2022. The 2021 Western North American Heatwave and Its Subseasonal Predictions. *Geophysical Research Letters* **49** (6): 1–10 DOI: 10.1029/2021GL097036

Lv Z, Pomeroy JW. 2020. Assimilating snow observations to snow interception process simulations. *Hydrological Processes* **34** (10): 2229–2246 DOI: 10.1002/hyp.13720

Magalhães N de, Evangelista H, Condom T, Rabatel A, Ginot P. 2019. Amazonian Biomass Burning Enhances Tropical Andean Glaciers Melting. *Scientific Reports* **9** (1): 1–12 DOI: 10.1038/s41598-019-53284-1

Malik MJ, van der Velde R, Vekerdy Z, Su Z. 2012. Assimilation of satellite-observed snow albedo in a land surface model. *Journal of Hydrometeorology* **13** (3): 1119–1130 DOI: 10.1175/JHM-D-11-0125.1

Marks D, Dozier J. 1992. Climate and energy exchange at the snow surface in the Alpine Region of the Sierra Nevada: 2. Snow cover energy balance. *Water Resources Research* **28** (11): 3043–3054 DOI: 10.1029/92WR01483

Marks D, Kimball J, Tingey D, Link T. 1998. The sensitivity of snowmelt processes to climate conditions and forest cover during rain-on-snow: a case study of the 1996 Pacific Northwest flood. *Hydrological Processes* **12** (10–11): 1569–1587 DOI: 10.1002/(SICI)1099-1085(199808/09)12:10/11<1569::AID-HYP682>3.0.CO;2-L

Marsh CB, Pomeroy JW, Wheater HS. 2020. The Canadian Hydrological Model (CHM) v1.0: a multi-scale, multi-extent, variable-complexity hydrological model - design and overview. *Geoscientific Model Development* **13** (1): 225–247 DOI: 10.5194/gmd-13-225-2020

Marshall SJ, Miller K. 2020. Seasonal and interannual variability of melt-season albedo at Haig Glacier, Canadian Rocky Mountains.*Cryosphere* **14** (10): 3249–3267 DOI: 10.5194/tc-14-3249-2020

McKenzie Skiles S, Flanner M, Cook JM, Dumont M, Painter TH. 2018. Radiative forcing by light-absorbing particles in snow. *Nature Climate Change* **8** (11): 964–971 DOI: 10.1038/s41558-018-0296-5

Menard CB, Essery R, Krinner G, Arduini G, Bartlett P, Boone A, Brutel-Vuilmet C, Burke E, Cuntz M, Dai Y, et al. 2021. Scientific and Human Errors in a Snow Model Intercomparison. *Bulletin of the American Meteorological Society* **102** (1): E61–E79 DOI: 10.1175/bams-d-19-0329.1

Milly PCD, Wetherald RT, Dunne KA, Delworth TL. 2002. Increasing risk of great floods in a changing climate. *Nature* **415** (6871): 514–517 DOI: 10.1038/415514a

Mishra AK, Singh VP. 2011. Drought modeling - A review. *Journal of Hydrology* **403** (1–2): 157–175 DOI: 10.1016/j.jhydrol.2011.03.049

Munro DS. 2004. Revisiting bulk heat transfer on Peyto Glacier, Alberta, Canada, in light of the OG parameterization. *Journal of Glaciology* **50** (171): 590–600 DOI: 10.3189/172756504781829819

Nash JE, Sutcliffe J V. 1970. River Flow Forecasting Through Conceptual Models Part I-a Discussion of Principles*. *Journal of Hydrology***10** : 282–290 DOI: 10.1016/0022-1694(70)90255-6

Newman R, Noy I. 2023. The global costs of extreme weather that are attributable to climate change. *Nature Communications* **14**(1) DOI: 10.1038/s41467-023-41888-1

Paniconi C, Putti M. 2015. Physically based modeling in catchment hydrology at 50: Survey and outlook. *Water Resources Research***51** (9): 7090–7129 DOI: 10.1002/2015WR017780

Parisien MA, Barber QE, Bourbonnais ML, Daniels LD, Flannigan MD, Gray RW, Hoffman KM, Jain P, Stephens SL, Taylor SW, et al. 2023. Abrupt, climate-induced increase in wildfires in British Columbia since the mid-2000s. *Communications Earth and Environment* **4** (1): 1–11 DOI: 10.1038/s43247-023-00977-1

Pietroniro A, Fortin V, Kouwen N, Neal C, Turcotte R, Davison B, Verseghy DL, Soulis ED, Caldwell R, Evora N, et al. 2007. Using the MESH modelling system for hydrological ensemble forecasting of the Laurentian Great Lakes at the regional scale. *Hydrology and Earth System Sciences* **3** (4): 1279–1294 DOI: 10.5194/hess-11-1279-2007

Pomeroy JW, Brown T, Fang X, Shook KR, Pradhananga D, Armstrong R, Harder P, Marsh C, Costa D, Krogh SA, et al. 2022. The cold regions hydrological modelling platform for hydrological diagnosis and prediction based on process understanding. *Journal of Hydrology***615** (October) DOI: 10.1016/j.jhydrol.2022.128711

Pomeroy JW, Fang X, Marks DG. 2016. The cold rain-on-snow event of June 2013 in the Canadian Rockies — characteristics and diagnosis.*Hydrological Processes* **30** (17): 2899–2914 DOI: 10.1002/hyp.10905

Pomeroy JW, Gray DM, Shook KR, Toth B, Essery RLH, Pietroniro A, Hedstrom N. 1998. An evaluation of snow accumulation and ablation processes for land surface modelling. *Hydrological Processes***12** (15): 2339–2367 DOI: 10.1002/(SICI)1099-1085(199812)12:15<2339::AID-HYP800>3.0.CO;2-L

Pradhananga D, Pomeroy JW. 2022. Diagnosing changes in glacier hydrology from physical principles using a hydrological model with snow redistribution, sublimation, firnification and energy balance ablation algorithms. *Journal of Hydrology* **608** (February): 127545 DOI: 10.1016/j.jhydrol.2022.127545

Pradhananga D, Pomeroy JW, Aubry-Wake C, Munro DS, Shea J, Demuth MN, Kirat NH, Menounos B, Mukherjee K. 2021. Hydrometeorological, glaciological and geospatial research data from the Peyto Glacier Research Basin in the Canadian Rockies. *Earth System Science Data* **13** (6): 2875–2894 DOI: 10.5194/essd-13-2875-2021

Queen LE, Mote PW, Rupp DE, Chegwidden O, Nijssen B. 2021. Ubiquitous increases in flood magnitude in the Columbia River basin under climate change. *Hydrology and Earth System Sciences* **25** (1): 257–272 DOI: 10.5194/hess-25-257-2021

Reichle RH. 2008. Data assimilation methods in the Earth sciences. *Advances in Water Resources* **31** (11): 1411–1418 DOI: 10.1016/j.advwatres.2008.01.001

Reichle RH, Walker JP, Koster RD, Houser PR. 2002. Extended versus ensemble Kalman filtering for land data assimilation. *Journal of Hydrometeorology* **3** (6): 728–740 DOI: 10.1175/1525-7541(2002)003<0728:EVEKFF>2.0.CO;2

Roujean JL, Leroy M, Dechamps PY. 1992. A Bidirectional Reflectance Model of the Earth's Surface for the Correction of Remote Sensing Data. *Journal of Geophysical Research* **97** (D18): 20455–20468 Available at: http://www.gps.caltech.edu/%5Cnvijay/Papers/BRDF/roujean-etal-92.pdf

Shuai Y, Masek JG, Gao F, Schaaf CB. 2011. An algorithm for the retrieval of 30-m snow-free albedo from Landsat surface reflectance and MODIS BRDF. *Remote Sensing of Environment* **115** (9): 2204–2216 DOI: 10.1016/j.rse.2011.04.019

Slater AG, Clark MP. 2006. Snow Data Assimilation via an Ensemble Kalman Filter. *Journal of Hydrometeorology* **7** (3): 478–493 DOI: 10.1175/JHM505.1

Smyth EJ, Raleigh MS, Small EE. 2020. Improving SWE Estimation With Data Assimilation: The Influence of Snow Depth Observation Timing and Uncertainty. *Water Resources Research* **56** (5): 1–17 DOI: 10.1029/2019WR026853

Tang G, Clark MP, Knoben WJM, Liu H, Gharari S, Arnal L, Beck HE, Wood AW, Newman AJ, Papalexiou SM. 2023. The Impact of Meteorological Forcing Uncertainty on Hydrological Modeling: A Global Analysis of Cryosphere Basins. *Water Resources Research* **59** (6): 1–31 DOI: 10.1029/2022WR033767

Thieken AH, Bubeck P, Heidenreich A, Von Keyserlingk J, Dillenardt L, Otto A. 2023. Performance of the flood warning system in Germany in July 2021 - insights from affected residents. *Natural Hazards and Earth System Sciences* **23** (2): 973–990 DOI: 10.5194/nhess-23-973-2023

Vermote EF, Tanré D, Deuzé JL, Herman M, Morcrette JJ. 1997. Second simulation of the satellite signal in the solar spectrum, 6s: an overview. *IEEE Transactions on Geoscience and Remote Sensing* **35** (3): 675–686 DOI: 10.1109/36.581987

Verseghy D. 2012. CLASS – The Canadian land surface scheme (version 3.6) - technical documentation. *Internal report, Climate Research Division, Science and Technology Branch, Environmental Canada* (February)

Wang T, Peng S, Krinner G, Ryder J, Li Y, Dantec-Nédélec S, Ottlé C. 2015. Impacts of satellite-based snow albedo assimilation on offline and coupled land surface model simulations. *PLoS ONE* **10** (9): 1–19 DOI: 10.1371/journal.pone.0137275

Wang Z, Erb AM, Schaaf CB, Sun Q, Liu Y, Yang Y, Shuai Y, Casey KA, Román MO. 2016. Early spring post-fire snow albedo dynamics in high latitude boreal forests using Landsat-8 OLI data. *Remote Sensing of Environment* **185** : 71–83 DOI: 10.1016/j.rse.2016.02.059

Wanner W, Li X, Strahler AH. 1995. On the derivation of kernels for kernel-driven models of bidirectional reflectance. *Journal of Geophysical Research* **100** (D10): 21077–21089 DOI: 10.1029/95JD02371

Warren SG, Wiscombe WJ. 1980. A Model for the Spectral Albedo of Snow. II: Snow Containing

Atmospheric Aerosols. *Journal of the Atmospheric Sciences* **37** (12): 2734–2745 DOI: 10.1175/1520-0469(1980)037<2734:AMFTSA>2.0.CO;2

Wheater HS, Pomeroy JW, Pietroniro A, Davison B, Elshamy M, Yassin F, Rokaya P, Fayad A, Tesemma Z, Princz D, et al. 2022. Advances in modelling large river basins in cold regions with Modélisation Environmentale Communautaire—Surface and Hydrology (MESH), the Canadian hydrological land surface scheme. *Hydrological Processes* **36** (4): 1–24 DOI: 10.1002/hyp.14557

Wiscombe WJ, Warren SG. 1980. A Model for the Spectral Albedo of Snow. I: Pure Snow. *Journal of the Atmospheric Sciences* **37**(12): 2712–2733 DOI: 10.1175/1520-0469(1980)037<2712:AMFTSA>2.0.CO;2

Wrzesien ML, Durand MT, Pavelsky TM, Howat IM, Margulis SA, Huning LS. 2017. Comparison of Methods to Estimate Snow Water Equivalent at the Mountain Range Scale: A Case Study of the California Sierra Nevada. *Journal of Hydrometeorology* **18** (4): 1101–1119 DOI: 10.1175/JHM-D-16-0246.1

Zhang Y, Kang S, Cong Z, Schmale J, Sprenger M, Li C, Yang W, Gao T, Sillanpää M, Li X, et al. 2017. Light-absorbing impurities enhance glacier albedo reduction in the southeastern Tibetan plateau. *Journal of Geophysical Research* **122** (13): 6915–6933 DOI: 10.1002/2016JD026397